



Contents lists available at ScienceDirect

Journal of Quantitative Spectroscopy & Radiative Transfer

journal homepage: www.elsevier.com/locate/jqsrt

Retrieval of HCFC-142b (CH₃CClF₂) from ground-based high-resolution infrared solar spectra: Atmospheric increase since 1989 and comparison with surface and satellite measurements

Emmanuel Mahieu^{a,*}, Bernard Lejeune^a, Benoît Bovy^a, Christian Servais^a, Geoffrey C. Toon^b, Peter F. Bernath^c, Christopher D. Boone^d, Kaley A. Walker^e, Stefan Reimann^f, Martin K. Vollmer^f, Simon O'Doherty^g

^a Institute of Astrophysics and Geophysics, University of Liège, Liège, Belgium

^b Jet Propulsion Laboratory, California Institute of Technology, Pasadena, CA, United States

^c Department of Chemistry and Biochemistry, Old Dominion University, Norfolk, VA, United States

^d Department of Chemistry, University of Waterloo, ON, Canada

^e Department of Physics, University of Toronto, ON, Canada

^f Empa, Laboratory for Air Pollution and Environmental Technology, Swiss Federal Laboratories for Materials Science and Technology, Switzerland

^g School of Chemistry, University of Bristol, UK

ARTICLE INFO

Article history:

Received 7 February 2016

Received in revised form

14 March 2016

Accepted 14 March 2016

Available online 18 March 2016

Keywords:

HCFC-142b

FTIR spectroscopy

Jungfraujoch

NDACC

ACE-FTS

AGAGE

ABSTRACT

We have developed an approach for retrieving HCFC-142b (CH₃CClF₂) from ground-based high-resolution infrared solar spectra, using its ν_7 band Q branch in the 900–906 cm⁻¹ interval. Interferences by HNO₃, CO₂ and H₂O have to be accounted for. Application of this approach to observations recorded within the framework of long-term monitoring activities carried out at the northern mid-latitude, high-altitude Jungfraujoch station in Switzerland (46.5°N, 8.0°E, 3580 m above sea level) has provided a total column times series spanning the 1989 to mid-2015 time period. A fit to the HCFC-142b daily mean total column time series shows a statistically-significant long-term trend of $(1.23 \pm 0.08 \times 10^{13} \text{ molec cm}^{-2})$ per year from 2000 to 2010, at the 2- σ confidence level. This corresponds to a significant atmospheric accumulation of (0.94 ± 0.06) ppt (1 ppt = 1/10¹²) per year for the mean tropospheric mixing ratio, at the 2- σ confidence level. Over the subsequent time period (2010–2014), we note a significant slowing down in the HCFC-142b buildup. Our ground-based FTIR (Fourier Transform Infrared) results are compared with relevant data sets derived from surface *in situ* measurements at the Mace Head and Jungfraujoch sites of the AGAGE (Advanced Global Atmospheric Gases Experiment) network and from occultation measurements by the ACE-FTS (Atmospheric Chemistry Experiment-Fourier Transform Spectrometer) instrument on-board the SCISAT satellite.

© 2016 Elsevier Ltd. All rights reserved.

1. Introduction

Ground-based Fourier Transform InfraRed (FTIR) instruments operated within the framework of NDACC (Network for the Detection of Atmospheric Composition Change, see <http://www.ndacc.org>) record broadband high-resolution solar spectra between ~ 2.3 and 14 μm , or 4350 and

* Correspondence to: Institute of Astrophysics and Geophysics – University of Liège – Quartier Agora, Allée du six Août, 19, B4000 – Liège (Sart Tilman) Belgique. Tel.: +32 4 366 97 86; fax: +32 4 366 97 47.

E-mail address: emmanuel.mahieu@ulg.ac.be (E. Mahieu).

715 cm^{-1} . This spectral range encompasses the signature of numerous tropospheric and stratospheric species (see e.g., Table 1 in [1]), including a suite of important halogenated source and reservoir gases, needed to monitor the success of the Montreal Protocol on the protection of stratospheric ozone and the Kyoto Protocol for the reduction of greenhouse gas emissions. Recent efforts have increased the number of such related FTIR targets, with additions of CCl_4 (carbon tetrachloride; [2]) and CF_4 (carbon tetrafluoride; [3]).

Hydrochlorofluorocarbons (HCFCs) are the first – and temporary – substitutes to the long-lived ozone-depleting halocarbons, in particular the anthropogenic chlorofluorocarbons (CFCs). Given the complete ban for emissive applications of the CFCs by the Montreal Protocol and its Amendments and Adjustments, HCFC emissions have been on the rise, with wide-spread use of these compounds in many applications, e.g., as foam blowing agents, in refrigeration and air-conditioning. While emissions of HCFC-22 (CHClF_2) remain by far the largest in this family with current levels close to 366 Gg yr^{-1} , annual emissions of HCFC-142b (CH_3CClF_2) reached a maximum close to 40 Gg yr^{-1} in the late 2000s. They have been decreasing since then down to $\sim 30 \text{ Gg yr}^{-1}$ in 2012 (see the HCFC142.csv electronic supplement of [4], and [5]). The global *in situ*/flask networks (Advanced Global Atmospheric Gases Experiment, AGAGE and the Earth System Research Laboratory of the National Oceanic and Atmospheric Administration, NOAA-ESRL) have monitored the evolution of the surface mole fraction of HCFC-142b over the last two decades, capturing an increase from a mean global concentration of 7 ppt (parts per trillion, 10^{-12} , or pmol mol^{-1}) in 1995, 12 ppt in 2000, 15 ppt in 2005. Carpenter and Reimann [5] report mean surface mole fraction of 21–22 ppt in 2012, with annual rate of increase of 0.4–0.5 ppt (or 2–2.4%) over 2011–2012. The lifetime of HCFC-142b has been re-evaluated at 18 years [6]; its global warming potential is 1980 on a 100-yr time horizon [7] and its ozone depletion potential 0.057 (Tables 5–2 in [8]).

The first detection of HCFC-142b in atmospheric infrared spectra has been reported by Dufour et al. [9], from solar occultation observations recorded by the ACE-FTS instrument (Atmospheric Chemistry Experiment-Fourier Transform Spectrometer on-board the SCISAT satellite; [10,11]). Using two strong features and two microwindows (from 1132.5 to 1136.5 cm^{-1} and 1191.5 to 1195.5 cm^{-1}), they determined rather constant vertical profiles between 8 and 18 km, both for 53°N and the tropical region. They noted a good agreement with surface mole fractions from the AGAGE station in Mace Head (53°N , Ireland), with a relative difference of less than 15% between the two data sets. Later, Rinsland et al. [12] derived the first ACE-FTS time series for the February 2004–August 2008 time period, focusing on another window spanning the 903 – 905.5 cm^{-1} spectral range. Mean annual trends of 0.9 and 1.2 ppt yr^{-1} were obtained for the 25 – 35°N and 25 – 35°S latitudinal belts, respectively, when considering ACE-FTS measurements in the 13–16 km altitude range. More recently, Brown et al. [13] reported trends for a suite of halogenated gases, using ACE-FTS occultation measurements performed in the tropical region during 2004–2010.

Relying on the same windows as Dufour et al. [9], they derived a mean increase of 1.17 ppt yr^{-1} ; they also identified an unexpected increase in the mixing ratio profile with altitude, up to 17 km, and attributed it to spectral interferences in the retrieval.

The purpose of this study is to report on the trend of the HCFC-142b total columns derived from high spectral resolution FTIR solar absorption spectra recorded at the Jungfraujoch station of the NDACC network. This site is located in the Swiss Alps, at 46.5°N latitude, 8.0°E longitude, 3580 m above sea level (a.s.l.). A total column time series has been derived using the ν_7 band Q branch near $11 \mu\text{m}$. The Jungfraujoch data set provides an independent measurement by remote-sensing of the HCFC-142b trend and our findings are compared with ACE-FTS and *in situ* time series available for similar Northern mid-latitudes.

2. The Jungfraujoch FTIR observations

Since the mid-1980s, infrared solar absorption spectra have been regularly recorded at the Jungfraujoch station under clear-sky conditions using very high-resolution (0.003 to 0.006 cm^{-1}) wide band-pass FTIR spectrometers. A set of optical filters combined with HgCdTe or InSb detectors are used in sequence to cover the mid-infrared spectral range. Two FTIR instruments have been in operation at this site, a homemade instrument from 1984 to 2008, and a commercial Bruker IFS-120HR spectrometer from the early 1990s to present. More information about the instrumentation used over the years is available in [1]. Here, we exploit spectra encompassing the 700 – 1400 cm^{-1} range and therefore several features of HCFC-142b near 904 , 967 , 1133 and 1194 cm^{-1} (see e.g., Fig. 2 in [14]). Their typical spectral resolution is 0.0061 cm^{-1} , corresponding to a maximum Optical Path Difference (OPD) of 81.97 cm (see Appendix A1 in [15]).

3. Analysis

It is clear from the literature that there are several HCFC-142b branches suitable for its retrieval from remote-sensing infrared measurements. As indicated in Section 2, previous studies [9,12,13] have adopted microwindows either near 904 cm^{-1} , or a combination of two intervals near 1133 and 1194 cm^{-1} . A band around 967 cm^{-1} is another potential candidate. However, if retrieving HCFC-142b is already a challenge using space-based occultation observations, then it is even more difficult from the ground because of the shorter atmospheric absorption path and stronger interferences, with enhanced absorptions by tropospheric gases such as water vapor (H_2O), carbon dioxide (CO_2), nitrous oxide (N_2O), even for the high-altitude Jungfraujoch site characterized by dry-air conditions.

A first step consisted in a careful inspection and comparison of the available bands, using representative simulations of the potential windows. The simulations were performed using HITRAN 2008 [16] for the line-by-line spectroscopic parameters, and pseudolines computed by

one of us (G.C.T.) from cross-section measurements for unresolved features (e.g., for the CFCs, HCFCs; see e.g., [17]). As for HCFC-142b, the pseudolines were adjusted to the cross-section spectra from Newnham and Ballard [14], considering measurements performed at temperatures ranging from 203 to 294 K between 870 and 1270 cm^{-1} (see [12]). For all species, mean vertical profiles deduced from version 6 of the WACCM (the Whole Atmosphere Community Climate Model; <http://waccm.acd.ucar.edu>, e.g., [18]) model predictions for the 1980–2020 period were used as *a priori*. Note however that for the simulations, the WACCM HCFC-142b profile was multiplied by 1.7 to get a total column of 2.3×10^{14} molec cm^{-2} while the water vapor profile was scaled such as to obtain a total column of 6.6×10^{21} molec cm^{-2} , corresponding to the median values for Jungfraujoch. The following spectral ranges were investigated: 900–906 cm^{-1} , 965–970 cm^{-1} , 1132–1136 cm^{-1} and 1191–1196 cm^{-1} . All simulations indicated that the HCFC-142b absorption remains very weak at 3.58 km a.s.l. Indeed, even when adopting an apparent solar zenith angle of 83.6°, we computed maximum HCFC-142b absorptions close to 1% at 1192.56 cm^{-1} , 0.7% at 1135.37 cm^{-1} , 0.5% at 904.9 cm^{-1} and 0.3% at 967.52 cm^{-1} . Of course, absorptions by nearby interferences have also to be carefully considered. It appears that the feature at 967 cm^{-1} is located in the wing of a strong CO_2 line and the one at 1135 cm^{-1} is in the wing of a saturated water vapor line. The situation looks more favorable for the 900–906 cm^{-1} and 1191–1196 cm^{-1}

windows. But independent fits to both domains have revealed that the second one leads to the determination of total columns systematically larger by more than 60%, with corresponding tropospheric mole fractions incompatible with *in situ* surface concentrations determined by the AGAGE and NOAA/ESRL networks. Fits of MkIV FTIR balloon spectra [19] also showed a bias between the two domains, but of $(35 \pm 10)\%$. The cause of this high bias remains unknown, but it is unlikely resulting from inconsistencies in the HCFC-142b cross-sections, since Le Bris and Strong [20], who compared their laboratory measurements and those of Newnham and Ballard [14], concluded that the integrated band strengths are in good agreement. Table 2 in [20] indicates mean relative deviations never exceeding 12% between the two sets for the relevant bands. Moreover, when fitting the set of pseudolines to the Newnham and Ballard [14] laboratory spectra in the 900–906 cm^{-1} , 1191–1196 cm^{-1} and a wide window covering 870–1270 cm^{-1} , the retrieved HCFC-142b amounts were all within 3% of each other. This supports the hypothesis that a missing interfering absorption is causing the bias, not the HCFC142b spectroscopy. Therefore and because of this significant bias, we decided to develop the ground-based retrieval strategy using only the ν_7 band Q branch.

Fig. 1 presents the simulation for the 900–906 cm^{-1} microwindow, adopting the settings described above and an OPD of 82 cm. Frame A shows the per-species spectra for the primary absorbers in this range, i.e. nitric acid

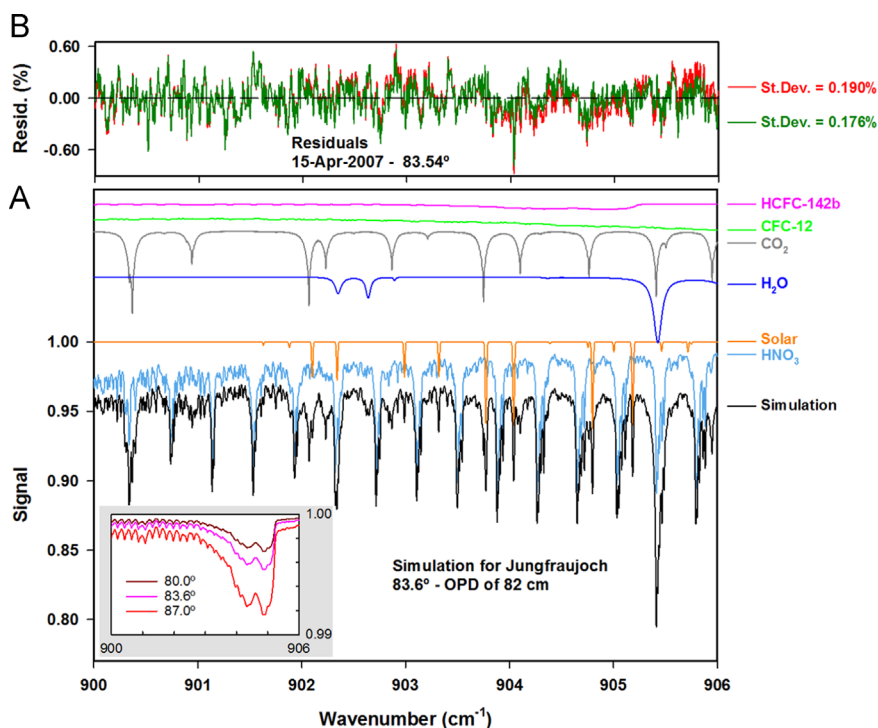


Fig. 1. Simulation of the 900–906 cm^{-1} spectral interval for the Jungfraujoch station with an apparent solar zenith angle of 83.6° and an OPD of 82 cm. The individual absorption spectra shown in frame A are color-coded and identified on the right-hand side. The HCFC-142b (CH_3CClF_2), CFC-12 (CCl_2F_2), CO_2 and H_2O spectra are offset vertically for clarity. The insert (bottom left) highlights the impact of the observing geometry on the depth of the HCFC-142b signal. Frame B displays typical residuals from the fit to a spectrum recorded on 15 April 2007, in green when including HCFC-142b in the retrieved species, in red when assuming no HCFC-142b in the atmosphere. (For interpretation of the references to color in this figure legend, the reader is referred to the web version of this article.)

(HNO₃), CO₂ and H₂O (see color code and their identification on the right-hand side). Next are the solar spectrum and the weaker absorptions by CFC-12 (CCl₂F₂, affecting the curvature of the continuum) and HCFC-142b. Note that the four uppermost traces have been shifted vertically for clarity. The continuous black line shows the resulting simulated spectrum, indicating a relatively clean window, even from the ground. The insert in frame A enlarges the HCFC-142b spectrum and shows the dependence of the absorption to the observing geometry, with simulations provided for three apparent zenith angles, 80°, 83.6° and 87°. With respect to the microwindow limits selected by Rinsland et al. (see Fig. 1 in [12]), we widened the range such as to fully include the absorption by the Q branch of HCFC-142b.

4. Retrieval settings, error budget and information content

The retrievals have been performed with the SFIT-2 v3.91 algorithm [21] which implements the Optimal Estimation Method (OEM) of Rodgers [22], using the standard 39-layer scheme for Jungfraujoch (see [23]), with the layer thicknesses progressively increasing from the site altitude (3.58 km) up to 100 km. In each layer, the mixing ratio of the target and interfering species as well as the mid-day pressure and temperature provided by the National Centers for Environmental Prediction (NCEP, Washington DC; see <http://www.ncep.noaa.gov>) are considered constant. The 900–906 cm⁻¹ microwindow was fitted using the (pseudo)line parameters mentioned in Section 3 and the set of mean vertical profiles from version 6 of the WACCM model simulations for 1980–2020. For HCFC-142b, the *a priori* mixing ratio profile is constant at 10.6 ppt in the whole troposphere, and then gradually decreases to 10 ppt at 13 km, 7 ppt at 22 km and 5 ppt at 30 km. The profiles of H₂O, CO₂ and CFC-12 are scaled on a per-spectrum basis during a pre-fit using two dedicated windows from 918.32 to 918.62 cm⁻¹ and 922.5 to 923.6 cm⁻¹. In the second run, the HCFC-142b profile is adjusted using a Tikhonov

type L1 regularization (see e.g., [24,25]). Vertical profiles were also retrieved for HNO₃ and H₂O. A further scaling of the CO₂ distribution was allowed while CFC-12 is held at the value deduced from the pre-fit.

Given the very low absorption of HCFC-142b, only the observations with an apparent zenith angle in the 80–87° range were fitted. 34 spectra from 2009 and 2010 with a representative distribution amongst the season and observing geometry have been selected to form a subset appropriate for the error budget calculations. As, for example, in [26], the formalism of Rodgers [22] has been applied to compute the gain and sensitivity matrices, allowing the measurement noise, smoothing and model parameter error terms to be determined. The Tikhonov regularization strength (the so-called alpha parameter) has been adjusted to minimize the resulting combined error, eventually setting the parameter at 25. Table 1 summarizes relative estimates of the major identified sources of random and systematic errors affecting our retrieved HCFC-142b total columns. The smoothing error was computed following Eq. (5) in [27], assuming a HCFC-142b atmospheric variability of 80% per km for the diagonal elements of the covariance matrix, and a Gaussian correlation length of 3 km for the extra-diagonal terms. The individual model parameters included the background slope and the wavenumber shifts for the telluric and solar lines. In addition to the random components computed thanks to the OEM formalism, we present other random and systematic mean contributions to the error budget evaluated by the perturbation method, using in this case all available observations from 2009 and 2010 (*i.e.* 242 spectra).

Measurement noise dominates the random errors, with a mean relative uncertainty of 18%, but individual values lie in the 12–26% range, notably dependent on the observing geometry (lower uncertainty for low-sun spectra) and water vapor column (lower uncertainty for dry observations). The next contributions are on the order of 3%, *i.e.* the smoothing, model parameter and temperature errors. The latter was determined by imposing temperature biases based on the NCEP estimates, which are function of altitude as follows: 1.5 K up to ~20 km, 2 K up to ~30 km, and from 5 to 9 K between 35 km and the stratopause. The

Table 1

Mean relative uncertainty affecting the total column retrieval of HCFC-142b (CH₃CClF₂), for the random and systematic components. See notes and text for information on how they were evaluated.

Error type and source	Relative uncertainty (%)	Notes
Random components		
Measurement noise	18	OEM formalism
Smoothing error	3	OEM formalism
Model parameters	3	OEM formalism
Temperature/pressure	3	Using the NCEP error pattern for T (see text for details)
<i>A priori</i> for water vapor	1	Adopting <i>a priori</i> with slopes divided/multiplied by 2 (see [26])
Sun-tracking geometry	2	Assuming ±0.1° for solar pointing
RSS total random	19	
Systematic components		
Forward model – retrieval algorithm	1	As per Duchatelet et al. [15]
HCFC-142b spectroscopy	6	Combining X-section uncertainty and conversion to pseudolines
Line parameters for main interfering species	6	Assuming HITRAN 08 uncertainties for HNO ₃ , H ₂ O and CO ₂
Instrumental line shape	< 1	± 10% misalignment
HCFC-142b <i>a priori</i> profile	1	Using ACE-FTS data
RSS total systematic	9	

RSS=square root of the sum of the squares.

uncertainty associated with pointing errors (2%) and with misrepresentation of the real slope in the *a priori* water vapor profile (1%) completes the random error budget. The latter, evaluated by adopting H₂O *a priori* profiles with slopes multiplied/divided by a factor two remains small, indicating that the water vapor gradient in the troposphere is appropriately determined in the second run.

The systematic error budget is mostly influenced by uncertainties associated with the spectroscopic parameters. For HCFC-142b, both the uncertainties affecting the cross-section measurements and their subsequent conversion into pseudolines have to be accounted for. Le Bris and Strong [20] provide a summary of the band strengths and associated errors (Table 2). For the ν_7 band, estimates of the associated errors by Le Bris and Strong [20] and Newnham and Ballard [14] are in the 2–3% range for the common temperatures of 233, 253 and 273 K. Moreover, comparison between the individual values available from these independent measurements shows a good consistency, with mean relative standard deviations at the three temperatures of 1.5%, 1.5% and 4%, respectively. A maximum error of 4% is associated with the conversion of cross-sections to pseudolines [12]. After combination in quadrature, we obtain a systematic uncertainty of 6% for the HCFC-142b parameters.

For the main interfering species, we assumed the maximum intensity errors quoted in HITRAN 2008, *i.e.* 30% for HNO₃, from 5% to 10% for H₂O and from 5% to 20% for CO₂. Impact on the retrieved HCFC-142b total columns has been evaluated for each of these species and we found that, once combined, they contribute 6% to the systematic error. The remaining sources of systematic error only marginally influence the total systematic error, with contributions of 1% (retrieval algorithm, *a priori* profile for HCFC-142b) or less (instrument alignment).

These evaluations led to total random and systematic uncertainties of 19% and 9%, commensurate with what we found for other weak absorbers (*e.g.*, [26,28]).

The information content has been characterized using the mean of all averaging kernels derived from the retrieval of the 2009–2010 spectra. Frame A of Fig. 2 shows the column averaging kernels for the first twelve individual layers (see color key) as well as for the total column (thick black line, scaled by 0.1), from the site altitude up to 30 km. The latter curve corresponds to the sensitivity of the retrieval (see *e.g.*, Section 2.3 in [29]), it is indicative of the fraction of information coming from the retrieval. The sensitivity remains close to the ideal value of 1 in the troposphere and lower stratosphere. The mean Degree Of Freedom for Signal (DOFS) is 1.01. The first eigen-vector of the column averaging kernel matrix is reproduced in frame B. It shows a maximum at the ground and a progressive decrease with altitude, with a half-maximum at 13 km. The corresponding eigen-value is close to 1, meaning that all the information characterizing the troposphere is coming from the retrieval. Since the second eigen-value is very small (~ 0.01), there is no height-resolution available (*e.g.*, [30]). The DOFS values show little dispersion, being all in the 1.00–1.03 range. We verified that these characteristics are confirmed when using other significant subsets of Bruker spectra; hence we are confident that the information content depicted in Fig. 2 is representative of the performance of the inversion developed and used here.

5. Results and discussion

All Bruker observations with apparent zenith angles in the 80–87° range recorded between January 2000 and

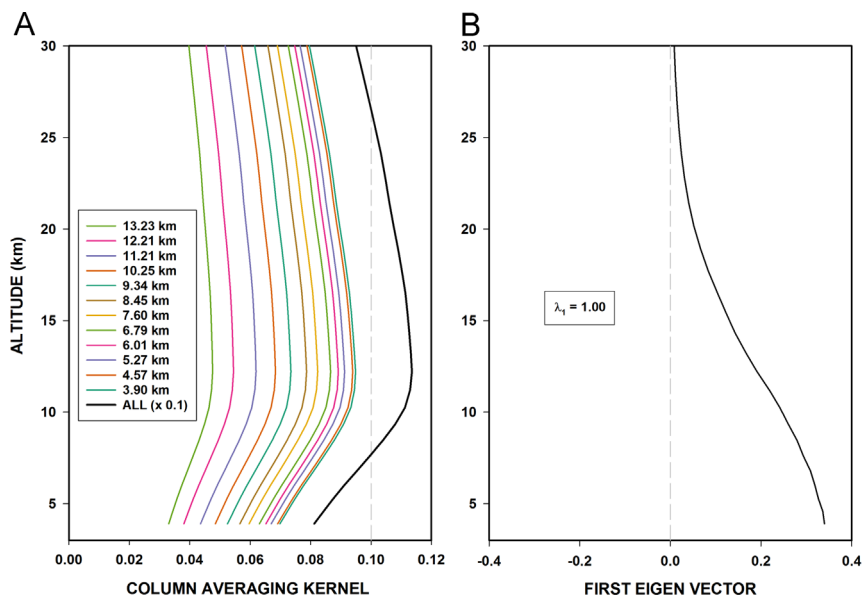


Fig. 2. Typical information content as derived from the mean of all column averaging kernels computed for the spectra from the years 2009 and 2010 (frame A) and corresponding first eigen-vector and value (frame B). The mean DOFS is 1.01, with only one piece of information available, essentially characterizing the tropospheric column of HCFC-142b (CH₃CClF₂).

the end of July 2015 have been fitted with the settings described in the previous section. The Jungfraujoch database includes 2046 Bruker spectra, with signal to noise ratios (S/N) mostly in the 470 to 1350 range (10th and 90th percentiles), with an average value of 910. The results derived from 1898 spectra were retained, covering 157 months and 621 different days. Causes for rejection include non-convergence of the fit, unusually poor residuals or low S/N. Typical residuals achieved can be seen in the green curve in frame B of Fig. 1, obtained for an observation with an apparent zenith angle and H₂O column close to the mean values for the time series (i.e. 83.5° for a mean of 83.6°; 6.36×10^{21} molec cm⁻² for a mean of 6.06×10^{21} molec cm⁻², respectively). The red curve shows the increase in residuals (by 8%; from 0.176% to 0.190%, for a retrieved HCFC-142b column of 2.29×10^{14} molec cm⁻²) when assuming no HCFC-142b in the atmosphere.

We investigated the possible correlation between the HCFC-142b and water vapor total columns as well as between the HCFC-142b total columns and the apparent zenith angle. In both cases, the scatter plots showed weak correlation, with *R* parameters of 0.3 and 0.1, respectively.

The monthly mean total columns were computed after normalization of all the individual columns to the standard pressure of 654 hPa (by multiplying the total column by the ratio of the standard pressure to the actual pressure, considering the closest pressure measurement at Jungfraujoch as provided every 10 min by MeteoSwiss). The Bruker time series from January 2000 until July 2015 is

displayed as blue symbols in Fig. 3, with the error bars reproducing the standard deviation around the monthly averages.

The first obvious feature is a significant increase of the HCFC-142b columns from 2000 until 2012, from yearly mean columns of 1.71×10^{14} molec cm⁻² in 2000 to 2.93×10^{14} molec cm⁻² in 2012, or a relative cumulative increase of 71%. Afterwards, the columns appear to progressively stabilize. Overall, the monthly mean columns present a noisy distribution, likely resulting from a difficult measurement affected by a large random uncertainty of 19%, on average. Note that the relative standard deviation around the monthly means amounts on average to 11%.

Because of a constrained Tikhonov regularization, the retrieved vertical distributions for HCFC-142b basically correspond to a homogeneous scaling of the *a priori* over the whole altitude range. Therefore, the correlation between the retrieved total columns and the tropospheric mixing ratios is extremely compact. Indeed, an *R* coefficient of 0.998 is computed, and a linear relationship allows for a direct conversion between the HCFC-142b total columns and the mixing ratios in the troposphere, with an error of less than 3% [3]. Comparison between the right- and left-axis scales in Fig. 3 provides the equivalence between the tropospheric mixing ratios and the total columns.

Our Bruker FTIR dataset is compared to HCFC-142b ground-based measurements at two AGAGE stations. Red crosses in Fig. 3 show monthly mean surface dry-air mole fractions derived at Mace Head (53°N, Ireland, see [31,32]),

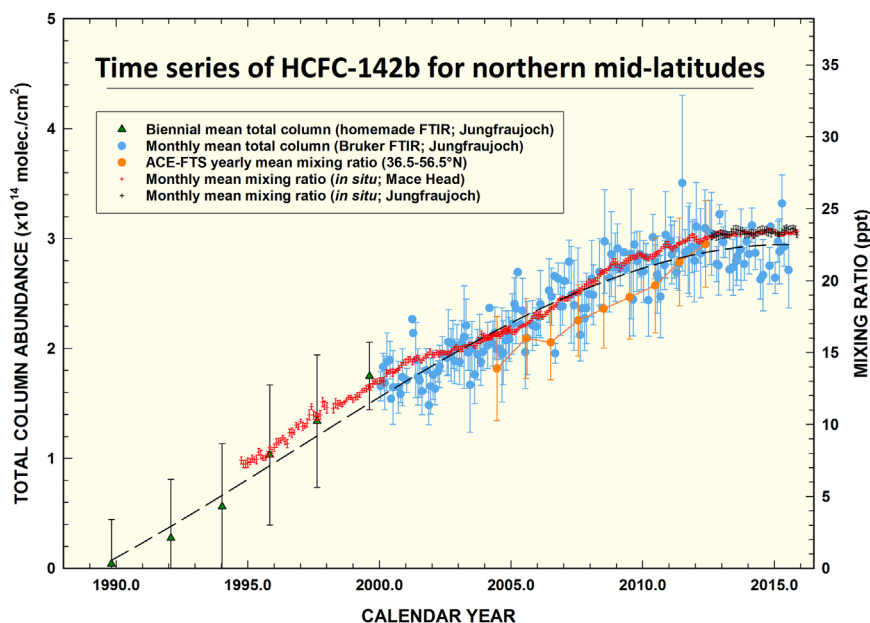


Fig. 3. Time series of HCFC-142b (CH₃CClF₂) for the northern mid-latitudes, as derived from infrared remote-sensing and *in situ* surface measurements. The blue circles show the Jungfraujoch FTIR monthly mean total columns retrieved from the Bruker solar spectra, from 2000 onwards. Earlier FTIR measurements performed with a homemade instrument have been combined as biennial mean total columns (see green triangles). The dashed line is a polynomial fit to both FTIR datasets. The right-hand axis provides the corresponding scale in term of mixing ratio (see text), allowing the direct comparison of the FTIR data with the yearly mean mixing ratios from ACE-FTS occultation measurements (orange circles) on-board SCISAT, between 36.5–56.5°N latitude and 14–18 km altitude; and with monthly mean dry-air surface mole fractions from the AGAGE stations at Mace Head (red crosses) and Jungfraujoch (black crosses). All vertical bars depict the standard deviations around the means (note that they are very small for the *in situ* datasets). (For interpretation of the references to color in this figure legend, the reader is referred to the web version of this article.)

with the GC–MS ADS system (Gas Chromatography–Mass Spectrometry Adsorption/Desorption System; [33]) for October 1994 until December 2004, and with the GC–MS Medusa system [34] for November 2003 until November 2015 (refer to right-hand vertical axis). The monthly averages considered here only include baseline measurements (also often referred to as background data measurements); pollution events have been filtered out. HCFC-142b surface mole fractions are also measured at Jungfraujoch with a Medusa instrument. Monthly mean baseline measurements from August 2012 to November 2015 are reproduced as black crosses. Both data sets are based on the Scripps Institution of Oceanography (SIO) SIO-05 primary calibration scale for HCFC-142b. The overall accuracy of these measurements is estimated at 4%. The records for the two AGAGE sites agree within their uncertainties for the overlapping time period.

We also considered HCFC-142b vertical profiles derived from ACE-FTS occultation measurements obtained from 2004 onwards in the 36.5–56.5°N latitudinal belt. Version 3.0/3.5 of the data set is used [35]. After a careful selection of the profiles (100 profiles with obvious outliers were discarded), the mixing ratios available from 2005 occultations recorded between March 2004 and October 2012 were averaged over monthly periods over the 14–18 km altitude range. This range was selected such as to avoid including mixing ratios biased low in the troposphere, where the HCFC-142b vertical distributions show an unrealistic increase with altitude attributed to spectral interferences in the retrievals [13]. For the 83 available months, we derived a mean relative standard deviation of 13%. For the sake of clarity, only the corresponding yearly mean mixing ratios are shown in Fig. 3, as orange circles.

The consistency among the various data sets has been evaluated by comparing yearly averaged mixing ratios, on the basis of fractional differences (FD; the ratio between the mixing ratios difference and their mean; see Eq. 2 in [36]). For the 2000–2014 time period, the FDs comparing the Mace Head *in situ* measurements and the FTIR tropospheric mixing ratios are in the –0.64% to 12% range (Mace Head – FTIR), with a mean value of $(3.9 \pm 3.2)\%$ ($1-\sigma$). When comparing the FTIR and ACE-FTS data, we determine a mean bias (ACE-FTS – FTIR) of $-(8 \pm 5)\%$. Finally, a mean difference of $(10 \pm 5)\%$ is obtained when comparing the Mace Head and ACE-FTS measurements (Mace Head – ACE-FTS). It is commensurate with the one reported in Dufour et al. [9], who quoted an agreement

better than 10% for mid-latitude measurements in March 2004 near 53°N.

The trends characterizing the various time series have been computed with the bootstrap resampling statistical tool described in [37], combining a linear function and a third-order Fourier series to account for the intra-annual variability of the data sets. Table 2 provides the annual trends derived for all subsets and selected time periods. Considering the FTIR daily mean columns available for the 2000–2010 time frame, we derived an annual column increase of $(1.23 \pm 0.08) \times 10^{13}$ molec cm⁻² ($2-\sigma$ uncertainty level), or $(7.6 \pm 0.5)\%/yr$, when taking the 2000.0 column as reference. The rates of change remain consistent for 2000–2011, 2000–2012 and 2000–2013. We only get a statistically different trend after addition of the 2014 data, confirming the recent slowing down in the HCFC-142b atmospheric accumulation, with a column change of $(1.04 \pm 0.05) \times 10^{13}$ molec cm⁻², or $6.1 \pm 0.3\%/yr$. When expressed in terms of mixing ratios, we obtain rates of increase of (0.94 ± 0.06) and (0.79 ± 0.04) ppt yr⁻¹ for 2000–2010 and 2000–2014, respectively. This compares well with the Mace Head trends derived for the same time intervals, *i.e.*, (0.86 ± 0.02) and (0.79 ± 0.02) ppt yr⁻¹, respectively, with no statistical differences at the $2-\sigma$ uncertainty level.

The trend derived for ACE-FTS over 2004–2012 is the largest of all, with a mixing ratio increase of (1.06 ± 0.09) ppt yr⁻¹. Such an increase is statistically compatible with the FTIR trend for 2000–2010. Although lower than the annual trend of 1.17 ± 0.05 ppt yr⁻¹ derived for 2004–2010 by Brown et al. [13] for the tropical regions, it is still higher than the *in situ* rate of change derived for Mace Head, in line with the disagreement noted in Carpenter and Reimann (see Table 1 and 2 and Section 1.2.1.5 in [5]). It is however important to point out that the atmospheric region sampled here (14–18 km between 36.5 and 56.5°N) by ACE-FTS primarily corresponds to the lower stratosphere, and in some instances to the upper troposphere. Indeed, statistics established with NCEP data covering the 1948–2015 time span [38] indicate mean tropopause heights of 13.4, 11.1 and 9.8 km for 35, 45 and 55°N, with mean seasonal modulations in the 11.3–15.3 km, 9.6–13 km and 8.9–10.9 km ranges, respectively. Given the time needed for tropospheric air parcels to reach and mix in the stratosphere, the ACE-FTS mixing ratios can reflect the state of the troposphere for up to 3 years earlier (see Fig. 2 in [39]; [3]; and references therein). Accounting for a mean stratospheric age-of-air of one year would

Table 2

Absolute annual trends for HCFC-142b (CH₃CClF₂) derived from the Jungfraujoch FTIR total column time series, from ACE-FTS occultation measurements in the 36.5–56.5°N latitude band and between 14 and 18 km altitude as well as from AGAGE *in situ* surface measurements at Mace Head and Jungfraujoch.

	2000–2010	2000–2014	2010–2014	2012–2015
Jungfraujoch FTIR	1.23 ± 0.08 E13 ^a	1.04 ± 0.05 E13 ^a	0.10 ± 0.30 E13 ^a	–
	0.94 ± 0.06 ppt/yr	0.79 ± 0.04 ppt/yr	0.05 ± 0.24 ppt/yr	–
ACE-FTS/SCISAT	1.06 ± 0.09 ppt/yr ^b	–	–	–
Mace Head <i>in situ</i>	0.86 ± 0.02 ppt/yr	0.79 ± 0.02 ppt/yr	0.36 ± 0.04 ppt/yr	0.10 ± 0.02 ppt/yr
Jungfraujoch <i>in situ</i>	–	–	–	0.08 ± 0.03 ppt/yr

^a Total column changes in molec cm⁻² per year.

^b Over 2004–2012.

reduce the systematic bias of $(10 \pm 5)\%$ noted above between ACE-FTS and Mace Head to $(6 \pm 4)\%$. As to the HCFC-142b increase rate, we will need to verify whether the correction in the upcoming version 4 of an improper CO₂ trend assumed in the current version of the ACE data base [40] will help to close this gap.

When considering the 2010–2014 time frame, we compute smaller $(0.36 \pm 0.04 \text{ ppt yr}^{-1}$ for Mace Head) or even non-significant trends $(0.05 \pm 0.24 \text{ ppt yr}^{-1}$ for the FTIR set), in line with reduced emissions of HCFC-142b from 2009 onwards [4]. Over the more recent 2012–2015 time period, the *in situ* time series indicate even smaller trends of $(0.10 \pm 0.02) \text{ ppt yr}^{-1}$ for Mace Head and $(0.08 \pm 0.03) \text{ ppt yr}^{-1}$ for the Jungfraujoch. Following the sharp rises observed until the end of the 2000s, the concentration of this replacement product, now close to 23.5 ppt, has almost stopped increasing in today's atmosphere.

In order to extend the time series back into the past and despite anticipated very low or near-zero absorption for the spectra recorded before 2000, the observations recorded with the homemade spectrometer from January 1989 to July 2000 have been systematically fitted, using the same approach as for the Bruker spectra. Since it is not possible to draw conclusions from the individual noisy measurements, we computed biennial column averages for 1989–1990, 1991–1992, and so on until 1999–2000. The averaged columns are shown as green triangles in Fig. 3, with the error bars depicting the standard deviations around the means. When considering together the Bruker and homemade FTIR monthly means, it is possible to characterize the overall evolution of HCFC-142b since late 1989 (see the polynomial fit in Fig. 3). An indicative trend of $1.2\text{--}1.3 \text{ ppt yr}^{-1}$ is determined for the 1990s.

6. Conclusions

We have established a strategy allowing the total columns of HCFC-142b (CH₃CClF₂) to be retrieved from ground-based high-resolution FTIR solar spectra. Among several candidate windows, the 900–906 cm⁻¹ domain encompassing its ν_7 band Q branch has been selected. This relatively clean window includes interferences by HNO₃, CO₂ and water vapor. Second order absorptions by the solar spectrum and CFC-12 must be accounted for.

This retrieval strategy enabled us to produce a multi-decadal total column time series, using FTIR spectra available from the high-altitude Jungfraujoch station (46.5°N). Given the weak absorptions by HCFC-142b, often lower than 1%, the retrievals have been limited to low-sun spectra, with apparent zenith angles in the 80–87° range. We evaluated that mean relative uncertainties of 19% (random) and 9% (systematic) affect the retrieved total columns.

The FTIR dataset has been compared to remote-sensing occultation measurements by the ACE-FTS instrument, considering upper-troposphere lower-stratosphere mixing ratios obtained in the 36.5–56.5°N latitudinal belt. We also included AGAGE monthly mean time series of background dry-air mole fractions from the Mace Head (53°N) and Jungfraujoch stations. All these independent HCFC-142b

data sets show good consistency, with relative differences well within the systematic uncertainty associated with the Bruker FTIR data. For ACE-FTS, the time needed for tropospheric air to reach the lower stratosphere should be accounted for.

The atmospheric accumulation of HCFC-142b from 2000 onwards has been characterized in terms of annual total column and mixing ratio increases, for selected time periods. Here again, we note a good overall agreement between the various datasets, and those extending after 2013 allow capturing the recent levelling off of HCFC-142b in today's atmosphere. For the 2000–2010 time period, we determined mean annual increases of 0.8–1.0 ppt yr⁻¹ (or $1.2 \times 10^{13} \text{ molec cm}^{-2}$ per year) while for 2010–2014, the rate of change dropped significantly to 0.1–0.4 ppt yr⁻¹ (or $0.1 \times 10^{13} \text{ molec cm}^{-2}$ per year). For the most recent years, atmospheric concentrations close to 23.5 ppt are measured at the AGAGE sites, with only a small change of 0.1 ppt yr⁻¹ over 2012–2015. This is more than 10 times lower than the trend derived for the 1990s from the early homemade FTIR measurements (1.2–1.3 ppt yr⁻¹).

For the near future, our intention is to pursue the development of retrieval approaches for additional atmospheric trace gases, in particular other CFC replacement products, to further augment the scope of the ground-based FTIR technique and to provide independent datasets useful for the characterization of changes affecting the composition of the Earth's atmosphere on the long-term. Given the characteristics of the HCFC-142b window selected here, we anticipate that our approach will be appropriate for the retrieval of HCFC-142b at other NDACC stations, allowing a global survey of this halogenated greenhouse gas with ground-based remote-sensing FTIR instruments.

Acknowledgments

The University of Liège involvement was primarily supported by the Belgian Federal Science Policy Office (BELSPO), through the AGACC-II project and the F.R.S – FNRS, both in Brussels. Emmanuel Mahieu is a Research Associate with the F.R.S. – FNRS. Additional support was provided by the GAW-CH program of MeteoSwiss. We further acknowledge the contributions of the Fédération Wallonie-Bruxelles for funding travel and subsistence costs to/at the Jungfraujoch station. We thank the International Foundation High Altitude Research Stations Jungfraujoch and Gornergrat (HFSJG, Bern) for supporting the facilities needed to perform the observations. We are grateful to the many Belgian colleagues who have performed the FTIR observations used here. Part of this work was conducted at the Jet Propulsion Laboratory, California Institute of Technology, under contract with NASA. The Atmospheric Chemistry Experiment (ACE), also known as SCISAT, is a Canadian-led mission supported primarily by the Canadian Space Agency.

Support for the GC-MS measurements at Jungfraujoch is provided to Empa by the Swiss National Program HAL-CLIM (Swiss Federal Office for the Environment, FOEN),

and by the HFSJG. The Fischer and Otz families are acknowledged for their on-site support at Jungfraujoch.

We thank the Physics Department, National University of Ireland, Galway, for making the research facilities at Mace Head available, and specifically the cooperation and efforts of the station operator, Mr Gerard Spain. The operation of the Mace Head station was supported by the Department of the Energy and Climate Change (DECC, UK) (Contracts GA0201 to the University of Bristol) and the National Aeronautic and Space Administration (NASA, USA) grants NNX07AE89G and NNX11AF17G to MIT.

This paper is dedicated to the memory of Prof. Rodolphe Zander who passed away unexpectedly on October 22, 2015. Among his many important scientific achievements, his contribution to the exploitation of the Jungfraujoch database has been tremendous. The Liège team members are grateful to him for his constant and strong support throughout the years, until well after his retirement, and will not forget the stimulating moments they have had the pleasure to share with him.

References

- Zander R, Mahieu E, Demoulin P, Duchatelet P, Roland G, Servais C, et al. Our changing atmosphere: evidence based on long-term infrared solar observations at the Jungfraujoch since 1950. *Sci Total Environ* 2008;391:184–95. <http://dx.doi.org/10.1016/j.scitotenv.2007.10.018>.
- Rinsland CP, Mahieu E, Demoulin P, Zander R, Servais C, Hartmann J-M. Decrease of the carbon tetrachloride (CCl₄) loading above Jungfraujoch, based on high resolution infrared solar spectra recorded between 1999 and 2011. *J Quant Spectrosc Radiat Transf* 2012;113:1322–9. <http://dx.doi.org/10.1016/j.jqsrt.2012.02.016>.
- Mahieu E, Zander R, Toon GC, Vollmer MK, Reimann S, Mühle J, et al. Spectrometric monitoring of atmospheric carbon tetrafluoride (CF₄) above the Jungfraujoch station since 1989: evidence of continued increase but at a slowing rate. *Atmos Meas Tech* 2014;7:333–44. <http://dx.doi.org/10.5194/amt-7-333-2014>.
- Rigby M, Prinn RG, O'Doherty S, Miller BR, Ivy D, Mühle J, et al. Recent and future trends in synthetic greenhouse gas radiative forcing. *Geophys Res Lett* 2014;41:2623–30. <http://dx.doi.org/10.1002/2013GL059099>.
- Carpenter LJ and Reimann S (Lead Authors), Burkholder JB, Clerbaux C, Hall BD, Hossaini R, Laube JC, Yvon-Lewis SA. Ozone-Depleting Substances (ODSs) and Other Gases of Interest to the Montreal Protocol. Chapter 1 in Scientific assessment of ozone depletion: 2014. Global ozone research and monitoring project – report no. 55. Geneva, Switzerland: World Meteorological Organization; 2014.
- SPARC. 2013: SPARC Report on the lifetimes of stratospheric ozone-depleting substances, their replacements, and related species. Ko MKW, Newman PA, Reimann S, Strahan SE, editors. SPARC report No. 6, WCRP-15/2013, available at www.sparc-climate.org/publications/sparc-reports/.
- IPCC. In: Stocker TF, Qin D, Plattner G-K, Tignor M, Allen SK, Boschung J, Nauels A, Xia Y, Bex V, Midgley PM, editors. *Climate Change 2013: the physical science basis. Contribution of working group I to the fifth assessment report of the intergovernmental panel on climate change*. Cambridge, United Kingdom and New York, NY, USA: Cambridge University Press; 2013. p. 1535.
- Harris NRP and Wuebbles DJ (Lead Authors), Daniel JS, Hu J, Kuijpers LJM, Law KS, Prather MJ, Schofield R. Scenarios and information for policymakers. Chapter 5 in Scientific assessment of ozone depletion: 2014. Global ozone research and monitoring project – report No. 55. Geneva, Switzerland: World Meteorological Organization; 2014.
- Dufour G, Boone CD, Bernath PF. First measurements of CFC-113 and HCFC-142b from space using ACE-FTS infrared spectra. *Geophys Res Lett* 2005. <http://dx.doi.org/10.1029/2005GL022422>.
- Bernath PF, McElroy CT, Abrams MC, Boone CD, Butler M, Camy-Peyret C, et al. Atmospheric Chemistry Experiment (ACE): mission overview. *Geophys Res Lett* 2005. <http://dx.doi.org/10.1029/2005GL022386>.
- Bernath PF. The atmospheric chemistry experiment (ACE), this issue; 2016.
- Rinsland CP, Chiou L, Boone C, Bernath P, Mahieu E. First measurements of the HCFC-142b trend from atmospheric chemistry experiment (ACE) solar occultation spectra. *J Quant Spectrosc Radiat Transf* 2009;110:2127–34. <http://dx.doi.org/10.1016/j.jqsrt.2009.05.011>.
- Brown AT, Chipperfield MP, Boone C, Wilson C, Walker KA, Bernath PF. Trends in atmospheric halogen containing gases since 2004. *J Quant Spectrosc Radiat Transf* 2011;112:2552–66. <http://dx.doi.org/10.1016/j.jqsrt.2011.07.005>.
- Newnham D, Ballard J. Fourier transform infrared spectroscopy of HCFC-142b vapour. *J Quant Spectrosc Radiat Transf* 1995;53:471–9. [http://dx.doi.org/10.1016/0022-4073\(95\)90047-0](http://dx.doi.org/10.1016/0022-4073(95)90047-0).
- Duchatelet P, Demoulin P, Hase F, Ruhnke R, Feng W, Chipperfield MP, et al. Hydrogen fluoride total and partial column time series above the Jungfraujoch from long-term FTIR measurements: Impact of the line-shape model, characterization of the error budget and seasonal cycle, and comparison with satellite and model data. *J Geophys Res* 2010;115. <http://dx.doi.org/10.1029/2010JD14677>.
- Rothman LS, Gordon IE, Barbe A, Benner DC, Bernath PF, Birk M, et al. The HITRAN 2008 molecular spectroscopic database. *J Quant Spectrosc Radiat Transf* 2009;110:533–72. <http://dx.doi.org/10.1016/j.jqsrt.2009.02.013>.
- Irion FW, Gunson MR, Toon GC, Chang AY, Eldering A, Mahieu E, et al. Atmospheric Trace Molecule Spectroscopy (ATMOS) Experiment Version 3 data retrievals. *Appl Opt* 2002;41:6968. <http://dx.doi.org/10.1364/AO.41.006968>.
- Chang L, Palo S, Hagan M, Richter J, Garcia R, Riggan D, et al. Structure of the migrating diurnal tide in the Whole Atmosphere Community Climate Model (WACCM). *Adv Space Res* 2008;41:1398–407. <http://dx.doi.org/10.1016/j.asr.2007.03.035>.
- Toon GC. The JPL MkIV interferometer. *Opt Photonics News* 1991;2:19. <http://dx.doi.org/10.1364/OPN.2.10.000019>.
- Le Bris K, Strong K. Temperature-dependent absorption cross-sections of HCFC-142b. *J Quant Spectrosc Radiat Transf* 2010;111:364–71. <http://dx.doi.org/10.1016/j.jqsrt.2009.10.005>.
- Rinsland CP, Jones NB, Connor BJ, Logan JA, Pougatchev NS, Goldman A, et al. Northern and southern hemisphere ground-based infrared spectroscopic measurements of tropospheric carbon monoxide and ethane. *J Geophys Res* 1998;103:28197. <http://dx.doi.org/10.1029/98JD02515>.
- Rodgers CD. *Inverse methods for atmospheric sounding: theory and practice (Series on atmospheric, oceanic and planetary physics)*, Vol. 2. Singapore: World Scientific Publishing Co.; 2000.
- Dils B, Cui J, Henne S, Mahieu E, Steinbacher M, De Mazière M. 1997–2007 CO trend at the high Alpine site Jungfraujoch: a comparison between NDIR surface in situ and FTIR remote sensing observations. *Atmos Chem Phys* 2011;11:6735–48. <http://dx.doi.org/10.5194/acp-11-6735-2011>.
- Sussmann R, Borsdorff T, Rettinger M, Camy-Peyret C, Demoulin P, Duchatelet P, et al. Technical Note: harmonized retrieval of column-integrated atmospheric water vapor from the FTIR network – first examples for long-term records and station trends. *Atmos Chem Phys* 2009;9:8987–99. <http://dx.doi.org/10.5194/acp-9-8987-2009>.
- Vander Auwera J, Fayt A, Tudorie M, Rotger M, Boudon V, Franco B, et al. Self-broadening coefficients and improved line intensities for the ν_7 band of ethylene near 10.5 μm , and impact on ethylene retrievals from Jungfraujoch solar spectra. *J Quant Spectrosc Radiat Transf* 2014;148:177–85. <http://dx.doi.org/10.1016/j.jqsrt.2014.07.003>.
- Franco B, Hendrick F, Van Roozendael M, Müller J-F, Stavrou T, Marais EA, et al. Retrievals of formaldehyde from ground-based FTIR and MAX-DOAS observations at the Jungfraujoch station and comparisons with GEOS-Chem and IMAGES model simulations. *Atmos Meas Tech* 2015;8:1733–56. <http://dx.doi.org/10.5194/amt-8-1733-2015>.
- Vigouroux C, Hendrick F, Stavrou T, Dils B, De Smedt I, Hermans C, et al. Ground-based FTIR and MAX-DOAS observations of formaldehyde at Réunion Island and comparisons with satellite and model data. *Atmos Chem Phys* 2009;9:9523–44. <http://dx.doi.org/10.5194/acp-9-9523-2009>.
- Dammers E, Vigouroux C, Palm M, Mahieu E, Warneke T, Smale D, et al. Retrieval of ammonia from ground-based FTIR solar spectra. *Atmos Chem Phys* 2015;15:12789–803. <http://dx.doi.org/10.5194/acp-15-12789-2015>.

- [29] Vigouroux C, Blumenstock T, Coffey M, Errera Q, García O, Jones NB, et al. Trends of ozone total columns and vertical distribution from FTIR observations at eight NDACC stations around the globe. *Atmos Chem Phys* 2015;15:2915–33. <http://dx.doi.org/10.5194/acp-15-2915-2015>.
- [30] Barret B, De Mazière M, Mahieu E. Ground-based FTIR measurements of CO from the Jungfraujoch: characterisation and comparison with in situ surface and MOPITT data. *Atmos Chem Phys* 2003;3:2217–23. <http://dx.doi.org/10.5194/acp-3-2217-2003>.
- [31] O'Doherty S, Cunnold DM, Manning A, Miller BR, Wang RHJ, Krummel PB, et al. Rapid growth of hydrofluorocarbon 134a and hydrochlorofluorocarbons 141b, 142b, and 22 from Advanced Global Atmospheric Gases Experiment (AGAGE) observations at Cape Grim, Tasmania, and Mace Head, Ireland. *J Geophys Res: Atmos* 2004;109. <http://dx.doi.org/10.1029/2003JD004277>.
- [32] Derwent RG, Simmonds PG, Grealley BR, O'Doherty S, McCulloch A, Manning A, et al. The phase-in and phase-out of European emissions of HCFC-141b and HCFC-142b under the Montreal Protocol: evidence from observations at Mace Head, Ireland and Jungfraujoch, Switzerland from 1994 to 2004. *Atmos Environ* 2007;41:757–67. <http://dx.doi.org/10.1016/j.atmosenv.2006.09.009>.
- [33] Simmonds PG, O'Doherty S, Nickless G, Sturrock GA, Swaby R, Knight P, et al. Automated gas chromatograph/mass spectrometer for routine atmospheric field measurements of the cfc replacement compounds, the hydrofluorocarbons and hydrochlorofluorocarbons. *Anal Chem* 1995;67:717–23. <http://dx.doi.org/10.1021/ac00100a005>.
- [34] Miller BR, Weiss RF, Salameh PK, Tanhua T, Grealley BR, Mühle J, et al. Medusa: a sample Preconcentration and GC/MS detector system for in Situ measurements of atmospheric trace halocarbons, hydrocarbons, and sulfur compounds. *Anal Chem* 2008;80:1536–45. <http://dx.doi.org/10.1021/ac702084k>.
- [35] Boone CD, Walker KA, Bernath PF. Version 3 retrievals for the atmospheric chemistry experiment fourier transform spectrometer (ACE-FTS). In: Bernath PF, editor. *The atmospheric chemistry experiment ACE at 10: a solar occultation anthology*. Hampton, Virginia, USA: A. Deepak Publishing; 2013. p. 103–27.
- [36] Strong K, Wolff MA, Kerzenmacher TE, Walker KA, Bernath PF, Blumenstock T, et al. Validation of ACE-FTS N₂O measurements. *Atmos Chem Phys* 2008;8:4759–86. <http://dx.doi.org/10.5194/acp-8-4759-2008>.
- [37] Gardiner T, Forbes A, de Mazière M, Vigouroux C, Mahieu E, Demoulin P, et al. Trend analysis of greenhouse gases over Europe measured by a network of ground-based remote FTIR instruments. *Atmos Chem Phys* 2008;8:6719–27. <http://dx.doi.org/10.5194/acp-8-6719-2008>.
- [38] NCEP (National Centers for Environmental Prediction) Global Reanalyses, (<http://www.esrl.noaa.gov/psd/thredds/catalog/Datasets/ncep.reanalysis.derived/tropopause/catalog.html?dataset=Datasets/ncep.reanalysis.derived/tropopause/pres.tropp.mon.mean.nc>); 2016 [accessed 02.02.16].
- [39] Diallo M, Legras B, Chédin A. Age of stratospheric air in the ERA-Interim. *Atmos Chem Phys* 2012;12:12133–54. <http://dx.doi.org/10.5194/acp-12-12133-2012>.
- [40] Harrison JJ, Chipperfield MP, Boone CD, Dhomse SS, Bernath PF, Froidevaux L, et al. Satellite observations of stratospheric hydrogen fluoride and comparisons with SLIMCAT calculations. *Atmos Chem Phys Discuss* 2015;15:34361–405. <http://dx.doi.org/10.5194/acpd-15-34361-2015>.